(i) What is the problem being addressed by the manuscript and why is it important to the Antennas & Propagation community? (limited to 100 words).

Multiple beam antennas embarked on communication satellites are key technology for high data rates and spectrum re-use. Typical antenna farm that produces a '4-color' coverage requires four dual-band reflector antennas in a single-feed-per-beam configuration. To reduce the number of antenna apertures, a new antenna architecture was proposed [7, 10]. This solution necessitates a dual-band dual polarisation reflection surface; although the proof of concept design of such a surface is shown in [7, 10], it is not practical due to the oversized unit cell. There has yet to appear any other design that can provide a practical solution to this antenna architecture. Here we propose a novel solution pertinent to this.

(ii) What is the novelty of your work over the existing work? (limited to 100 words).

This paper introduces a novel periodic reflecting surface which provides dual-band orthogonal polarization conversion while maintaining unit cell dimensions below the critical grating lobe limit of half wavelength. This is the first design of its kind with dimensions that ensure no grating lobes occur for any angle of incidence. This property is of high significance in multiple beam antenna applications, where the surface will unavoidably be illuminated from several angles simultaneously.

(iii) Provide up to three references, published or under review, (journal papers, conference papers, technical reports, etc.) done by the authors/coauthors that are closest to the present work. Upload them as supporting documents if they are under review or not available in the public domain. Enter "N.A." if it is not applicable.

N. J. G. Fonseca and C. Mangenot, "Low-profile polarizing surface with dual-band operation in orthogonal polarizations for broadband satellite applications," *in 8th Eur. Conf. Antenna Propag.(EUCAP), 2014*.

N. J. G. Fonseca and C. Mangenot, "High-performance electrically thin dual-band polarizing reflective surface for broadband satellite applications," IEEE Trans. Antenna Propag., vol. 64, no. 2, pp.640-649, 2016.

E. Doumanis, G. Goussetis, J.L.Gomez-Tornero, R. Cahill and V. Fusco, "Anisotropic impedance surfaces for linear to circular polarization conversion," IEEE Trans. Antenna Propag., vol. 60, no. 1, pp.212-219, 2012.

(iv) Provide up to three references (journal papers, conference papers, technical reports, etc.) done by other authors that are most important to the present work. Enter "N.A." if it is not applicable.

K.Karkkainen,M. Stuchly, "frequency selective surface as a polarization transformer," IEE Proc. Microwave Antenna Propag., vol. 149, no. 516, pp.248-252, 2002.

G.Maral and M.Bousquet, "Satellite communications systems, systems, techniques and technology," Sussex,U.K. Wiley, 2009.

C.Mangenot and W.A.Imbriale, "Space antenna challenges for future mission, key techniques and technologies (Chapter 18)," in space antenna handbook, John Wiley & Sons Ltd, U.K, 2012.

Low-Profile Compact Dual-Band Unit Cell for Polarizing Surfaces Operating in Orthogonal Polarizations

Wenxing Tang, Salvador Mercader-Pellicer, George Goussetis, Herve Legay, and Nelson J.G. Fonseca

***Abstract*—This paper introduces a novel periodic reflector which provides linear to circular polarization conversion in two frequency bands. Significantly, the reflector converts a slant 45° linearly polarized wave into two orthogonal circular polarizations over two separate frequency bands while further the unit cell dimensions are maintained below the critical grating lobe limit of half wavelength. Unlike previous designs providing this performance, which are based on linear dipole elements, miniaturization is here achieved by exploiting resonances in both TE and TM polarized waves. The operating principle of the polarizer is discussed and a parametric study is presented to derive design guidelines. A prototype working in the satellite Ku band has been designed and tested to validate the proposed design. The proposed polarizer can find applications in multiple beam satellite antenna systems in order to reduce the number of reflector apertures in a single-feed-per-beam configuration.**

***Index Terms*—Multiple-beam reflector antenna, dual-band polarization, polarization conversion, frequency selective surface, satellite communications.**

I. Introduction

Broadband satellite communications have been attracting significant attention in recent years [1, 2]. Multiple beam antennas embarked on communication satellites are a key underpinning technology to provide high data rates and spectrum re-use efficiency with an approach equivalent to terrestrial cellular networks. The typical multiple beam antenna farm for a '4-color' frequency and polarization re-use scheme requires four dual-band reflector antennas in a single-feed-per-beam (SFB) configuration [3]. The advantages of this configuration are high gain, low side lobe level and excellent carrier over interference ratio. However, this solution leaves no room for secondary missions as the two lateral faces of a satellite are occupied by the primary mission antenna farm. Significant efforts have over the past few years been dedicated on the development of antenna components and architectures that will enable reflector re-use in multiple beam missions [4-14].

From an electromagnetic point of view, the need for four dual-band reflector antennas to achieve a '4-color' coverage can be understood since contiguous multiple spot beam coverage from the same reflector requires feeds that physically overlap as illustrated in Fig.1 where the feed horn in red is to cover beam spot B, but, it is overlapped with the feed horns in blue which cover beam spot A. Since this is not practically feasible, beams generated by a single main reflector are angularly separated (by approximately an angle equal to the beamwidth of one beam) in all radial directions. Full contiguous coverage therefore necessitates four main reflectors and their corresponding feed clusters that produce interleaved beams in all directions [3].

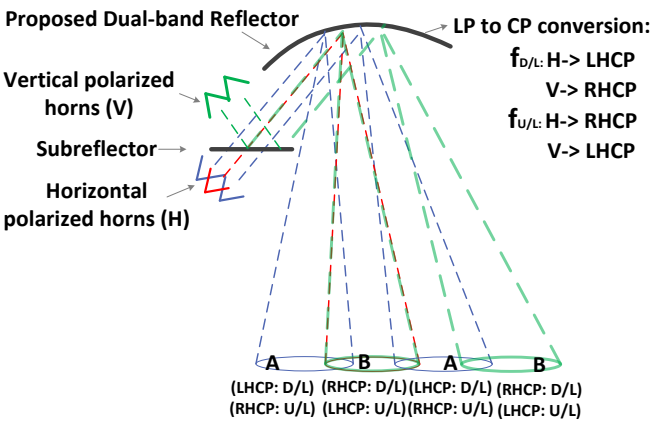

Fig. 1. Illustration of problem for contiguous multibeam coverage in Single Feed per Beam configuration; for contiguous beams "A" and "B", the blue and red feeds physically overlap. The proposed scheme exploits a linear polarization (e.g. wire grid) selective subreflector and a dual-band orthogonal linear to circular main reflector to enable the feeds associated with beams "B" to be at a physically different location.

One solution to reducing the number of main reflectors exploits multiple-feed-per-beam (MFB) configurations. In this approach, each beam is generated by a cluster of feeds. Contiguous coverage from the same reflector is possible by virtue of re-using some feeds between adjacent clusters. Existing MFB solutions enable a full transmit/receive coverage with only two apertures [4-5]. Despite the fact that more compact dual band MFB arrays have recently been developed [6], this class of solutions usually increases the complexity of the feed system and in particular the complexity of the beam forming network (BFN) [4] and degrades the RF performance when compared to equivalent SFB configurations.

An alternative solution to reducing the number of main reflectors while maintaining an SFB configuration is to combine two different feed clusters on a same main reflector using a quasi-optical diplexing sub-reflector. Considering that frequency re-use is based on adjacent frequency bands without guard band, frequency diplexing is ruled out. The remaining option is related to polarization re-use and is based on polarization selective sub-reflector solutions. Examples of optical devices which can be exploited for linear polarization (LP) diplexing include the wire grid subreflector diplexer [7] or the dual gridded reflector [8]. Circular polarization (CP)

Manuscript received March 03, 2016. This work was supported by the European Space Agency, under contract no. 4000107415 and FP7 project DORADA (IAPP-2013-610691).

W. Tang, S. Mercader-Pellicer and G. Goussetis are with the Institute of Sensors Signals and Systems, Heriot-Watt University, Edinburgh, EH14 4AS, UK (e-mail: w.tang@hw.ac.uk, g.goussetis@ieee.org).

H. Legay is with the Research and Development Department, Thales Alenia Space, 31037 Toulouse, France (herve.legay@thalesaleniaspace.com).

N.J.G. Fonseca is with Moltek Consultants Ltd for the European Space Agency, Antenna and Sub-Millimetre Wave Section, Keplerlaan 1, 2200 AG, Noordwijk, The Netherlands (nelson.fonseca@esa.int).

diplexing is also in principle attainable [9-10] although circular polarization selective surfaces are less mature and not as highly performing as their LP counterparts with the main restriction being the operating frequency bandwidth.

Despite the conceptual opportunities for reflector re-use by virtue of quasi-optical polarization diplexing, engineering challenges to implement such a solution relate to the requirement for orthogonal circular polarization (CP) for a given beam over the down- and up-links, which at Ka-band occur across two different frequency bands separated by a ratio of 1:1.5. In particular, the use of the same reflector for collimating both the down- and up-link beams necessitates a similar illumination across the two frequency bands in terms of amplitude and phase distribution but in orthogonal CPs. Since in a SFB scenario both Rx and Tx beams originate from the same feed, the optical path between feed and reflector should therefore be the same for the two beams. Hence a polarization diplexing configuration based on a gridded sub-reflector can only operate on the basis of down- and up-link beams being generated with the same polarization at the feed. The critical item for the implementation of this solution is therefore a polarizing main reflector that converts the same incoming LP into two orthogonal CPs at the down- and up-link bands respectively as illustrated in Fig. 1. This is the core underlying concept in the novel solution recently proposed in [11].

Broadband low-profile polarizing surface that converts LP to CP have been introduced recently [12, 13]. Both designs achieve 3 dB axial ratio fractional bandwidth in excess of 60%, which is sufficient for the entire Ku- or Ka-band frequency range. These designs, however, only provide the same polarization over transmit and receive bands and therefore are not compatible with the antenna farm described in [11]. To overcome this limitation, Fonseca and Mangenot [11, 14] proposed a new approach to design a low-profile polarizing surface with dual-band operation in orthogonal polarizations. The design, supported by experimental results [14], is based on periodic dipole arrays. Since closed form expressions for the equivalent impedance of this class of periodic surfaces are available [15], the synthesis procedure of the polarizer proposed in [11, 14] is relatively straightforward. Despite such attractive features, the longest unit cell dimension in [11, 14] is 0.94 wavelengths (0.94 λ_0) at the higher operating frequency. This feature makes the design liable to grating lobes even at very low angles of incidence [16].

To overcome grating lobe limitations, we propose a new and compact dual-band reflection polarizer design operating in orthogonal polarizations that is schematically depicted in Fig. 2. The proposed design provides operation comparable to [11, 14] but now all unit cell dimensions are lower than half wavelength (< 0.5 λ_0), and therefore no visible grating lobes occur at any angle of incidence. By examining the reflection phase characteristics of each orthogonal linear polarisation, this paper reviews the operating principle of the polariser proposed in [11, 14] and highlights the fundamental aspects that enable miniaturisation exploiting the structure of Fig. 2. Parametric studies are presented to provide design guidelines and the concept is experimentally validated by means of a fabricated breadboard.

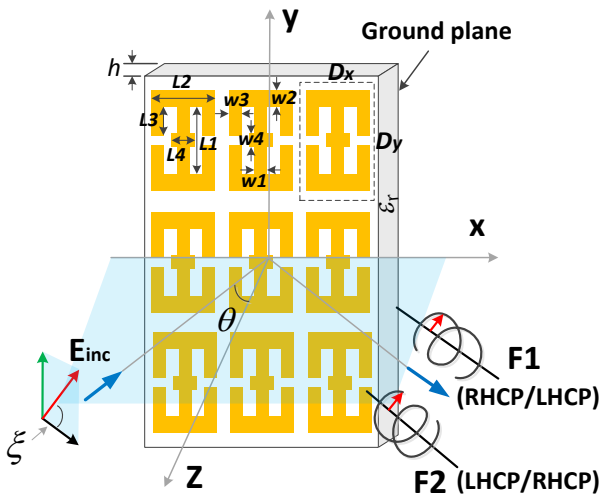

Fig. 2. Geometrical configuration and operation principle.

II. Operating Principle and Analysis

A. Operating principle

Reflection polarizers discussed above comprise a printed periodic array on a grounded substrate. The combined engineered surfaces (i.e. grounded substrate and periodic array) present an equivalent impedance that depends on the array element geometry [17]. In the lossless case, the magnitude of the reflection coefficient from the combined structure is unity. Therefore on the Smith chart the equivalent impedance of the combined surface lies on the circle with $|\Gamma|= 1$. Within the usual Smith chart terminology, the combined surface will therefore exhibit inductive/capacitive impedance when the reflection phase is positive/negative. Due to the finite thickness of the dielectric substrate and the dispersive characteristics of the periodic array, the equivalent impedance of the combined surface will vary with frequency. A zero of the equivalent impedance occurs when passing from capacitive to inductive regions while a pole occurs when passing from inductive to capacitive. We further note that for anisotropic arrays, the equivalent impedance for each polarization is different.

LP to CP conversion is achieved by means of providing a ±90° (or odd multiple of) phase difference between two incident orthogonal linear polarizations [12, 13]. In order to achieve orthogonal CPs at two distinct frequency ranges for a same incident slant LP, the dual-band design in [11, 14] exploits the inductive regime for both polarizations in the lower band and the capacitive regime for both polarizations in the higher band. This is schematically depicted in Fig. 3a, where the reflection phase for normally incident LP plane waves parallel (here conventionally noted as TE mode and marked red line) and perpendicular (noted as TM mode, blue line) to the dipoles for the design of [11, 14] is reproduced.

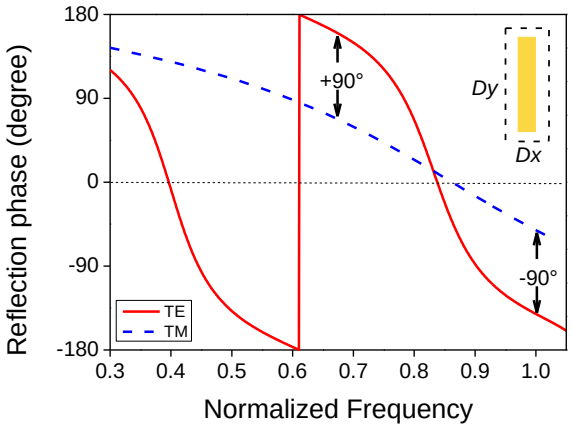

(a)

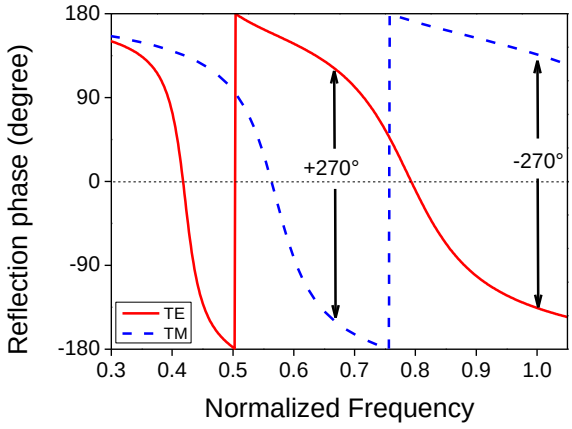

(b)

Fig. 3. Reflection phase sketches under normal LP incidence of (a) the design in [11] (inset: its unit cell) and (b) the proposed design.

Note that in Fig. 3a the frequency axis is normalized to the higher operating frequency, 30 GHz in this specific case. As shown, the equivalent impedance for both polarizations exhibits a pole between the lower and the upper band. Orthogonal CPs over the two bands is achieved due to the TM reflection phase varying slower with frequency than the TE reflection phase, leading to phase lag/lead compared to the resonant TE wave between the two bands.

The operating principle of the polarizer in [11, 14] is therefore based on two conditions, namely that; a) the boundary condition experienced on the periodic array by the TM polarization is weak (so that the reflection phase for this polarization varies slowly with frequency), and; b) the combined surface operates beyond the second resonance of the TE polarization (so that the TE equivalent impedance lies in the same inductive/capacitive half circle of the Smith chart as the TM one). The first condition suggests that the element geometry is very narrow along one direction. As a result, the second condition necessitates an element that is approximately one wavelength long (so that it exhibits both the half and full wavelength resonances within the operating frequency range) in the orthogonal direction. This leads to the approximately one-wavelength dipole of [11, 14].

Instead of exploiting a pole for both LPs between the two operating frequency bands, here we propose introducing a zero/pole for the TE/TM modes respectively. As a result, the proposed polarizer operates on an inductive/capacitive regime for TE/TM modes in the lower band and a capacitive/inductive regime for TE/TM polarizations in the higher band. This is illustrated in Fig. 3b, for the Ku-band design presented in section III. The design is compatible with commonly encountered D/L and U/L frequency plans in the Ku band and to facilitate comparison with Fig. 3a, the horizontal axis is also normalized to the higher operating frequency, here 18 GHz.

Significantly, this operation is compatible with resonances for both TE and TM polarizations. Although it is still required that the second resonance of the TE mode is within the operating frequency range, introducing a resonance for the TM polarization miniaturizes the unit cell due to the effective loading of the array element [18]. It is noted that since the ratio of the U/L to D/L frequencies for Ku and Ka band plans is approximately equal to 1.5, the two designs of Fig. 3 are comparable. In light of this comparison, it can be seen that the proposed approach enables to reduce the length and the profile of the polarizer's unit cell to nearly half of the one in [11]. It is noted that as a side consequence of the miniaturization, the fractional bandwidth of the proposed polarizer is reduced but still meets the typical requirement of Ku & Ka band missions.

B. Parametric analyses and design guidelines

An attractive feature of the proposed element geometry (Fig. 2) is that, to a first approximation, it enables to almost independently adjust the reflection properties for each polarization. This is due to the fact that different geometrical features have stronger impact on the reflection properties of each mode. This is here demonstrated by virtue of numerical results and parametric studies, which enable to derive design guidelines that ultimately minimize the computational cost of the final optimization.

With reference to the geometry shown in Fig.2, the parametric studies are performed around baseline dimensions as follows: *L1*=6.5 mm, *L2*=3.5 mm, *L3*=3.0 mm, *L4*=1.0 mm, *Dy*=8.0 mm, *Dx*=4.0 mm. The width, *w*, is 0.5 mm for all lines. For simplicity perfect electric conductor (PEC) is used for the metallic layers with an associated thickness of 17 μm. The substrate is considered lossless with relative permittivity ε_r=3.5 and thickness *h*=1.524 mm. Full-wave EM simulations have been performed using CST microwave studio [19] to analyze the reflected differential phases of TE and TM waves against various geometrical parameters. Steps of -0.5 mm to +0.5 mm are used around the baseline dimensions for the analyses. In the remaining the structure is analyzed under normally incident linearly polarized TE and TM wave excitations.

Fig. 4 (a) illustrates the variations of reflection phases under TE and TM waves excitation against dimensions *Dy* and *L1* (both varying simultaneously). It shows that only the TE phase is affected while the TM phase remains nearly constant. Interestingly, the opposite occurs when dimensions *Dx* and *L2* are varied as shown in Fig. 4 (b). The phase of the TM wave is shifted down as *Dx* and *L2* increase while the TE phase remains nearly constant. These results suggest that the design over the

upper frequency band is mainly dependent on *Dy* and *L1* while for the lower frequency band, *Dx* and *L2* are the key parameters to be tuned. Both TE and TM phase can be changed as the substrate thickness *h* varies as shown in Fig. 4 (c). It is interesting that the TE phase becomes more parallel to the TM phase when *h* increases, indicating a wider bandwidth of the two frequency bands could be achieved when a thicker substrate is employed. The dimensions of middle stub (*L4*, *w4*) can be used to finely adjust the upper frequency band while leaving the lower frequency band untouched as depicted in Fig. 4 (d). As can be seen, only the phase of the TM wave at high frequencies is changing when *L4* varies. This is particularly useful to reduce the separation between the two frequency bands by increasing *L4*.

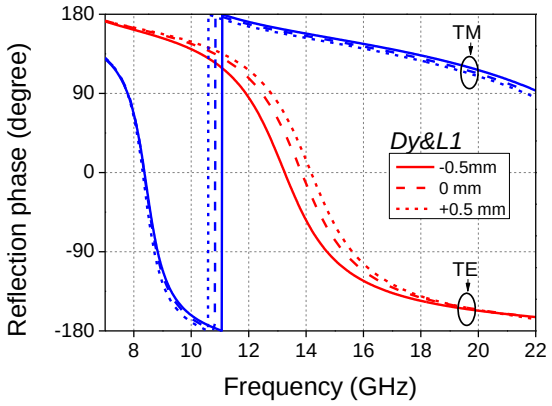

(a)

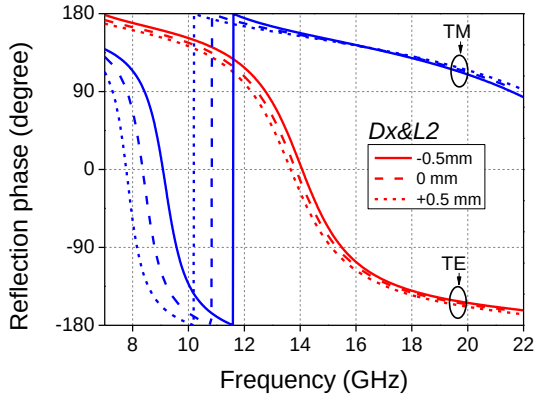

(b)

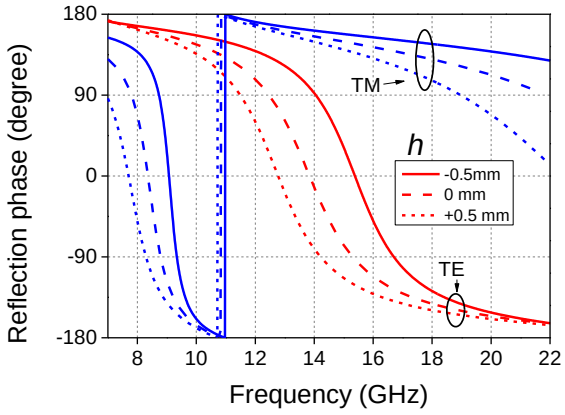

(c)

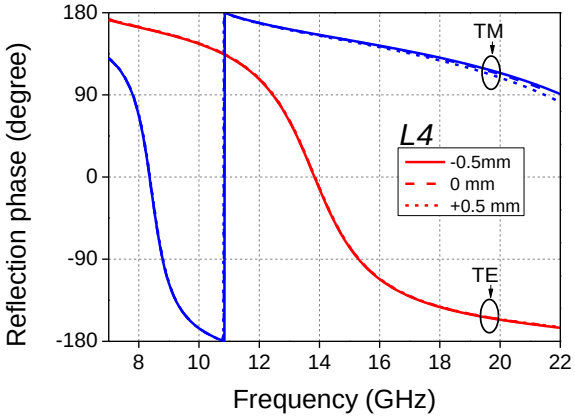

(d)

Fig. 4. Reflection TE and TM phase vary against (a) *Dy*&*L1*. (b) *Dx*&*L2*. (c) *h*. (d) *L4*. Baseline dimensions: *L1*=6.5 mm, *L2*=3.5 mm, *L3*=3.0 mm, *L4*=1.0 mm, *Dy*=8.0 mm, *Dx*=4.0 mm, and *w*=0.5 mm for all lines. Substrate: ε_r=3.5, *h*=1.524 mm.

According to the analysis above, an efficient design procedure for the proposed dual-band dual-polarization polarizer is as follows. Firstly it is noted that the proposed geometry can be seen as two split-rings with gaps along the y-axis connected back-to-back so that they share the segment noted as *L1*. Since this element is required to provide a second order resonance within the frequency range of interest, the initial length of the split-ring (without considering the capacitive loading of the gap) is chosen at one wavelength at the center of the upper frequency band. The width of the ring is selected to be compatible with fabrication tolerances. Next, *Dy* and *Dx* are chosen to pack the split-rings closely. This ensures the first resonance of the TE and TM modes vary gradually against frequency [20], which is preferred for wide bandwidth design. An empirical first-order rule is that *Dx* be chosen about half *Dy*. Finally, parameters sweep can be performed to adjust the phase of the TE and TM modes for the two frequency bands following the guidelines derived from Fig. 4.

III. Prototype And Experimental Validation

Based on the design guidelines discussed above, a Ku band polarizer operating in orthogonal polarizations has been developed covering frequency ranges of 11.7 - 12.5 GHz and 17.3 - 18.1 GHz. Full-wave simulation has been performed using CST microwave studio [19]. The final dimensions obtained from the design procedure outlined in section II and some final optimization are (in mm): *L1*=5.35, *L2*=3.31, *L3*=2.58, *L4*=1.86, *w1*=1.3, *w2*=0.4, *w3*=0.6, *w4*=0.5, *h*=1.524, *Dx*=3.9, *Dy*=8.0. The substrate parameters are ε_r=3.5, $tan\delta$ =0.0035 while copper of thickness 17 μm is assumed for the metallic layers. The reflection coefficients and phases of the TE and TM mode are plotted in Fig. 5 under normal incidence. As shown, the differential reflection phases over the two frequency bands are +270° and -270° respectively, which indicates the conversion to orthogonal CP in each of the two bands. Both reflection coefficients are better than -0.2 dB in the bands of interest. The axial ratio obtained by this response for a slant 45° polarized incidence is shown in Fig. 6(c). As shown, the axial

ratio is better than 0.36 dB over the two frequency bands.

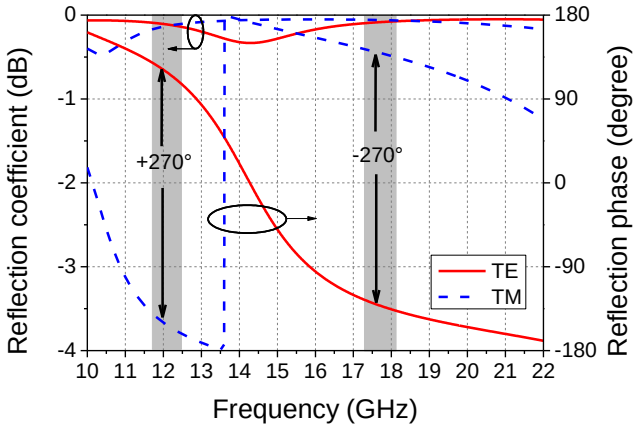

Fig. 5. Reflection coefficient and phase response under normal incidence.

The angular performance of the designed polarizer is given in Fig. 6. It shows that the axial ratio is better than 1.9 dB for incident angles up to 30° in the xz-plane. In the yz-plane, the axial ratio maintains good performance only up to 15° with an axial ratio better than 1.0 dB. The degraded performance in yz-plane is attributed to the fact that the periodicity of the polarizer is larger in that plane (*Dy*>*Dx*). However this represents significant improvement compared to the design proposed in [11, 14], where angles of incidence up to 2° are sufficient to degrade the performance. Significantly, since the unit cell dimensions are less than half wavelength, no grating lobes occur for this design at any angle of incidence. It is therefore possible to optimize the geometry of each unit cell for a given angle of incidence in order to minimize the axial ratio. In antenna architectures with a wider range of locally incidence angles, this can lead to a quasi-periodic array design according to reflectarray principles for global axial ratio miniaturization.

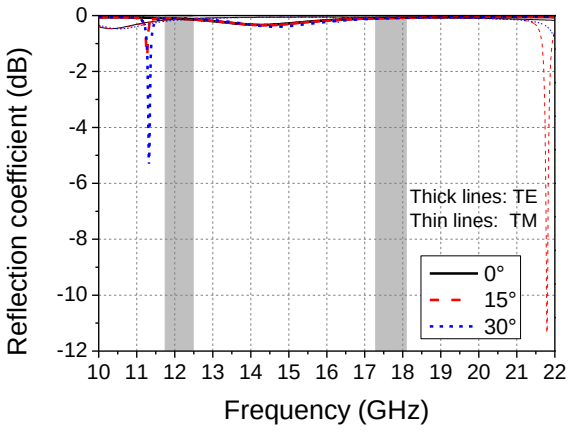

(a)

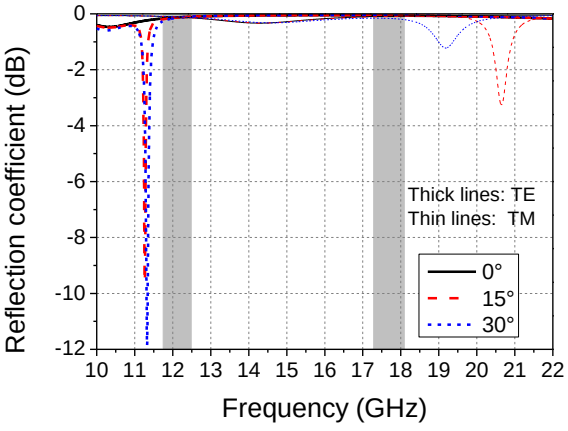

(b)

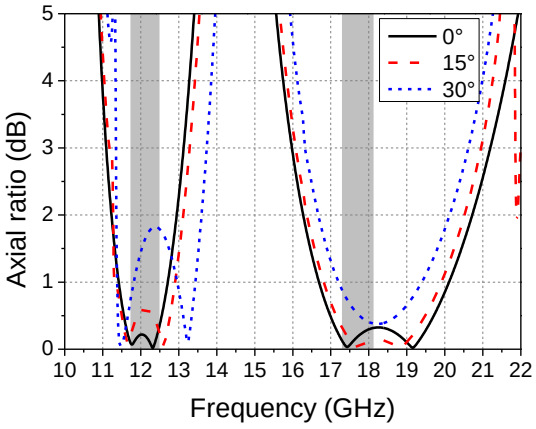

(c)

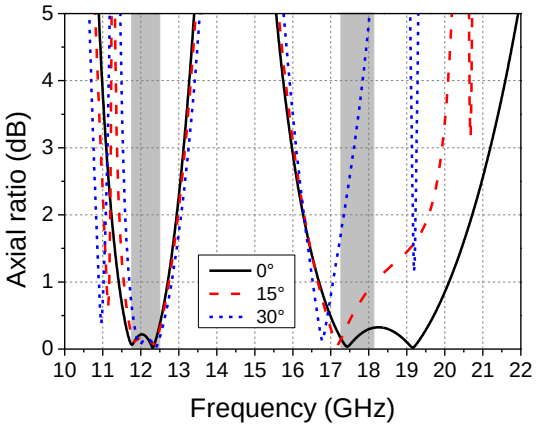

(d)

Fig. 6. Reflection coefficient and axial ratio under oblique incidence. (a, c) Incident angle varies in xz-plane. (b, d) Incident angle varies in yz-plane.

As reported in previous work [14], some peaks of absorption are also identified here at oblique incidence, which are thought to be associated to surface wave or cavity effects. The main difference with respect to previous work is that in the proposed design, these peaks appear both in the xz- and yz-plane, which is consistent with the fact that the periodicity along the xz-plane, *Dx*, is larger in this design than in previous work, but still remains below the worst case which is along the y-axis

(yz-plane). The complexity of the proposed unit cell makes it more difficult to identify the cause of these resonances and predict the frequency of the peak of absorption. Still, it can be seen from the numerical results provided in Fig. 6(a), (b) that these peaks remain outside the operating band over the considered angular range and thus are not the primary cause for axial ratio degradation.

In order to validate the proposed dual-band polarizer, a prototype has been fabricated and tested. The array has been photo-etched on one side of a Taconic RF-35 laminate [21] with the other side left for grounding. The laminate has a relative dielectric permittivity ε_r =3.5, loss tangent $tan\delta$=0.0035 and thickness of h=1.524 mm. A photograph of the fabricated breadboard is shown in Fig. 7a. The fabricated polarizer consists of 50 x 72 unit cells with overall size of approximately 45 cm x 30 cm including mounting margin.

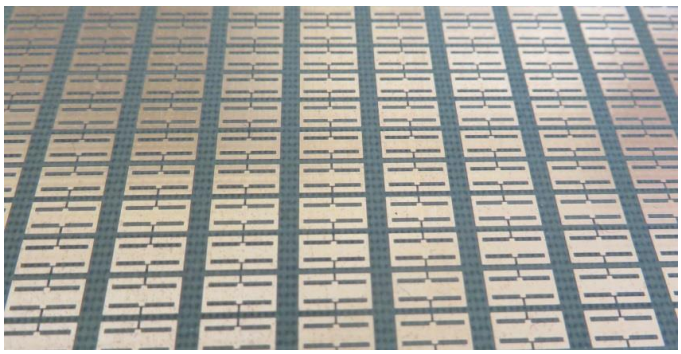

(a)

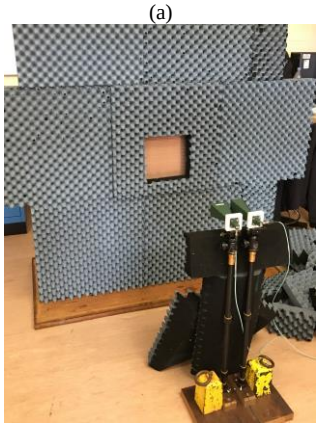

(b)

Fig. 7. Fabricated proposed dual-band polarizing surface (a) and (b) Measurement setup.

The measurements were performed using a vector network analyzer (PNA N5225A) with the measurement setup given in Fig.7b. Two linearly polarized rectangular pyramidal standard gain horn antennas are connected to port 1 and port 2 of the VNA, respectively, and placed on the same side to form a bistatic configuration with a very low incidence angle (about 2°). Two sets of standard horn antennas were used to cover the two frequency bands, operating in the ranges 10 to 15 GHz and 15 to 22 GHz respectively. The array was supported surrounded by radar absorbing materials (RAM). The distance between the horns and the array was chosen to ensure the array was in the far field. For measuring 10 - 15GHz, the distance was 110 cm while for 15 - 22GHz it was 80 cm. The measurement was normalized with the array replaced by a metallic plate of the same size. Co-polar complex reflection coefficients were measured with both horns vertically placed for TE incidence, while for TM incidence, both horns were rotated by 90°. For cross-polar measurement, one horn was rotated by 90° with respect to the other.

The axial ratio calculated from the measured complex reflection coefficients up to 21 GHz is plotted in Fig. 8, where the equivalent simulated response is produced for comparison.

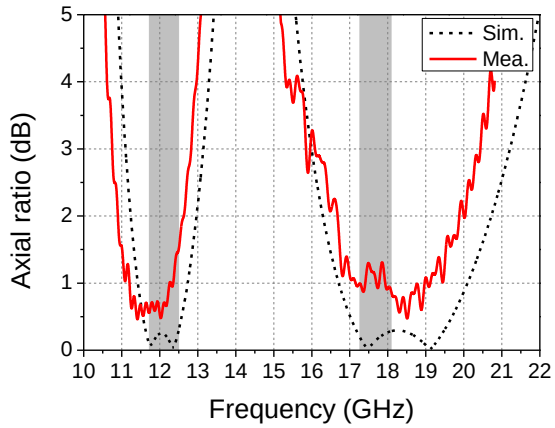

Fig. 8. Comparison of measured and simulated axial ratio performance under an incident angle of 2° in xz-plane. (noted that bistatic horns configuration was utilized in the measurement)

Good agreement between the measured and simulated results can be observed. The measured response is slightly shifted to lower frequencies when compared to the simulated results. In addition, there is about 0.5 dB differences between the measured and simulated axial ratio. These discrepancies are attributed to the material loss tolerance, fabrication tolerance, and also the experimental setup tolerance such as horn alignment and reference plane alignment.

IV. Conclusion

A novel low-profile compact unit cell polarizing surface has been presented that converts a given linearly polarized wave into two orthogonal circularly polarized waves over two frequency bands. This design can find pertinent application in multibeam satellite missions. The operation principle of the polarizer has been discussed and design guidelines were drawn based on the operation principle and the parametric studies. A design example compatible with typical Ku-band multibeam satellite missions together with measurements were presented. The agreement observed between the measured and simulated results validates the proposed concept.

Acknowledgment

The authors would like to thank Dr. Cyril Mangenot, from the European Space Agency, for valuable recommendations in connection with this topic of research and Taconic Advanced Dielectric Division for providing the laminates.

REFERENCES

[1] G.Maral and M.Bousquet, "Satellite communications systems, systems, techniques and technology," Sussex,U.K. Wiley, 2009.

[2] C.Mangenot and W.A.Imbriale, "Space antenna challenges for future mission, key techniques and technologies (Chapter 18)," in space antenna handbook, John Wiley & Sons Ltd, U.K, 2012.

[3] S.K. Rao, "Parametric design and analysis of multiple-beam reflector antennas for satellite communications," IEEE Antenna Propag. Magazine, vol. 45, no. 4, pp.26-34, Aug. 2003.

[4] M. Schneider, C. Hartwanger, E. Sommer and H. Wolf, "The multiple spot beam antenna project Medusa," 3rd European conf. antenna propag. (EuCap), pp. 726-729, 2009.

[5] M. Schneider, C. Hartwanger and H. Wolf, "Antennas for multiple spot beam satellites," German Aerospace Congress, Bremen, Germany, Sep. 2011.

[6] P. Bosshard, "THALES ALENIA SPACE : HTS/V-HTS Multiple Beam Antennas Sub-systems on the Right Track, in 10th Eur. Conf. Antenna Propag.(EUCAP), 2016.

[7] E. Vourch, *et al.*, "Ku-multibeam antenna with polarization grids," IEEE AP-S Int. Symp., Jun. 2007, Honolulu, Hawaii, pp. 5183-5186.

[8] M. Baunge, H. Ekstrom, P. Ingvarson and M. Petersson, "A new concept for dual gridded reflectors," *in 4th Eur. Conf. Antenna Propag.(EUCAP), 2010*.

[9] J. Sanz-Fernandez, E. Saenz, and P. de Maagt, "A Circular polarization selective surface for space applications," *IEEE Trans. Antenna Propag.*, vol. 63, no. 6, pp. 2460-2470, Jun. 2015.

[10] W.Tang, G.Goussetis, H.Legay,N.J.G.Fonseca, E. Sáenz and P.d.Maagt, "Coupled split-ring resonator circular polarization selective surface," submitted to IEEE Transactions Antennas and Propagation.

[11] N. J. G. Fonseca and C. Mangenot, "Low-profile polarizing surface with dual-band operation in orthogonal polarizations for broadband satellite applications," *in 8th Eur. Conf. Antenna Propag.(EUCAP), 2014*.

[12] K.Karkkainen,M. Stuchly, "frequency selective surface as a polarization transformer," IEE Proc. Microwave Antenna Propag., vol. 149, no. 516, pp.248-252, 2002.

[13] E. Doumanis, G. Goussetis, J.L.Gomez-Tornero, R. Cahill and V. Fusco, "Anisotropic impedance surfaces for linear to circular polarization conversion," IEEE Trans. Antenna Propag., vol. 60, no. 1, pp.212-219, 2012.

[14] N. J. G. Fonseca and C. Mangenot, "High-performance electrically thin dual-band polarizing reflective surface for broadband satellite applications," IEEE Trans. Antenna Propag., vol. 64, no. 2, pp.640-649, 2016.

[15] N. Marcuvitz, "Waveguide handbook," Peter Peregrinus Ltd., London, 1993.

[16] B.A.Munk, "Frequency selective surface, theory and design," New York,USA. Wiley, 2000.

[17] M. García-Vigueras, J.L. Gómez-Tornero, G. Goussetis, J.S. Gómez-Díaz, and A. Álvarez-Melcón, "A Modified Pole-Zero Technique for the Synthesis of Waveguide Leaky-Wave Antennas Loaded with Dipole-Based FSS," IEEE Transactions on Antennas and Propagation, Vol. 58, No. 6, pp. 1971-1979, June 2010

[18] G. Goussetis, Y. Guo, A. P. Feresidis, and J. C. Vardaxoglou, "Miniaturised and Multiband Artificial Magnetic Conductors and Electromagnetic Band Gap Surfaces", IEEE AP-Symposium 2004, Monterey CA, 2004

[19] "Microwave Studio user's manual, version 2015" CST AG, 2015.

[20] J.-J.Sanz-Fernandez, R. Cheung, G. Goussetis, C. Mateo-Segura, "Power Stored and Quality Factors in Frequency Selective Surfaces at THz Frequencies," *IEEE Transactions on Antennas and Propagation*, Vol. 19, No. 6, pp. 2205-2216.

[21] "RF-35 data sheet", 2010, NY, USA, Taconic Corporation.